Electrical Power and Energy Systems 97 (2018) 418–427

Contents lists available at ScienceDirect

Electrical Power and Energy Systems

journal homepage: www.elsevier.com/locate/ijepes

Transient stability of a distribution subsystem during fault-initiated switching to islanded operation

Wei Zheng[a,*], Peter Crossley[a], Bingyin Xu[b], Haijie Qi[c]

[a] School of Electrical and Electronic Engineering, The University of Manchester, Manchester, UK
[b] School of Electrical and Electronic Engineering, Shandong University of Technology, Zibo, China
[c] University of Strathclyde, Glasgow, UK

ARTICLE INFO

Keywords:
Distributed generation
Fault-initiated islanding
Induction motor loads
Load shedding
Transient stability

ABSTRACT

This paper investigates the transient stability of a load-rich distribution subsystem during the switching process to islanded mode instigated by a permanent fault. When operating in islanded mode, the subsystem must maintain a generation-load power balance and use at least one distributed generator (DG) to regulate the system frequency and voltage. Therefore, switching control must be executed after the disconnection of the main grid and a strategy which includes a DG coordination method and a single-step load shedding scheme is proposed. Other factors also have a substantial impact on the system transient performance, including the type of subsystem load, the DG penetration level, the fault clearance time and the switching control delay. To perform the study, a distribution subsystem was simulated using PSCAD/EMTDC software, consisting of a mix of synchronous and inverter-based DGs and a combination of static loads and dynamic motor loads. Simulation results show the proposed switching control strategy can effectively ensure successful switching from grid-connected to islanded mode under different fault conditions and DG penetration levels.

1. Introduction

Increasing use of distributed generation in utility distribution networks has encouraged researchers to consider intentional islanding. Intentional islanding normally happens as a consequence of routine switching or pre-designed protective actions against grid faults [1,2]. Current utility practices, such as IEEE Std. 1547-2003 [3], do not normally permit islanding operation and require all downstream DG units to be disconnected after the grid supply fails due to a fault. The exception is during routine maintenance or when a pre-designed microgrid is deliberately operated in islanded mode. This requirement is imposed to address safety concerns and to comply with the existing control and protection constraints of distribution networks [4]. However, to fully utilise the benefits of DG technology, such as maintaining uninterrupted service and offering high quality and reliable power to customers, autonomous islanded operation needs to be considered. As a result, the IEEE Std. 1547-2003 and IEEE Std. 1547.4-2011 [5] suggest intentional islanding is an important task for future consideration.

An islanding-possible system should contain a cluster of DGs which are capable of operating in either grid-connected or islanded mode and switching between these modes when required [6]. Immediately after the disconnection of the main grid, the islanded subsystem will experience rapid and severe frequency and voltage deviations. The intensity of these deviations depends on various factors, including the type of DGs and their control approaches, the type of load, the DG penetration level, the severity of the fault that triggers islanding, the fault clearance time and the switching control delay.

Fault-initiated switching from grid-connected to islanded mode was investigated previously in [6–8]. However, all these studies were conducted on pre-designed generation-sufficient microgrids, i.e. the installed generation capacity exceeds the local load demand. Paper [2] studied a load-rich microgrid, but only considered inverter-based DG and constant impedance loads. In this study, the amount of load shedding was analytically computed based on the voltage change rate and proved effective in ensuring a successful transition. Islanding events triggered by various types of fault were studied in [7], and in this scenario, the microgrid included a mix of synchronous and inverter-based DGs. Paper [8] investigated the transient behaviour of induction motor (IM) loads during an islanding event triggered by a three-phase fault, and used the critical clearing time to evaluate the transient stability of the microgrid. In the aforementioned papers, inverter-based DGs were assumed to be fully dispatchable and can participate in the system frequency regulation using their rapid response to smooth the transients during the transition process.

* Corresponding author.
E-mail address: wei.zheng-6@postgrad.manchester.ac.uk (W. Zheng).

https://doi.org/10.1016/j.ijepes.2017.11.024
Received 28 August 2017; Received in revised form 31 October 2017; Accepted 19 November 2017
0142-0615/

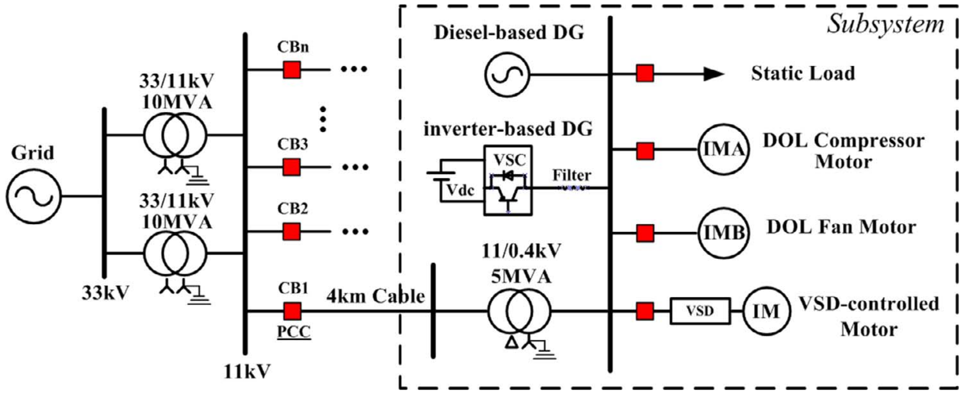

Fig. 1. Single line layout of the distribution system under study.

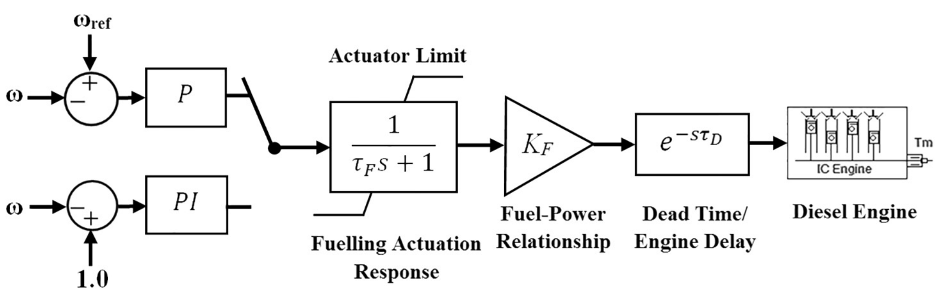

Fig. 2. Diesel engine governor model.

Load shedding priority is another critical factor affecting the transient performance of a load-rich subsystem during the islanding switching process. Load shedding priority has been extensively investigated, which can be determined by either technical or social reasons, such as voltage stability indicators [9], customers' willingness to pay [10] and the dynamically computed critical nature of the load [11]. In this paper, load shedding priority is designed based on the transient stability of different types of load during the fault-initiated islanding. IM's dynamics when experiencing a fault induced voltage dip was studied in [8,12,13]. The main emphasis of [8] was the stability of microgrids with or without IM loads. Three- and single-phase IMs were analytically evaluated in [12,13] respectively. Motor stalling phenomenon can be seen in both types of motor, which may result in delayed voltage recovery and other stability issues.

When the switching control strategy proposed in this paper is applied, real time simulations were conducted on various scenarios to validate the reliability of the strategy. The major contributions of this paper include: (1) comprehensive research into the electromagnetic transients during the islanding switching initiated by various types of fault, (2) assessment of a single-step load shedding scheme designed to ensure successful islanding switching of a load-rich subsystem containing motor loads, and (3) analysis of the other factors that might affect the system transient stability during the switching process, including the DG penetration level, the fault clearance time and the switching control delay.

Clarification of the scope of this paper is important for future researches. First, the results are specific to a subsystem consisting of a mix of synchronous and inverter-based DG. Second, the subsystem is load-rich and the maximum active power generation available from the DG units is 40–80% of the total subsystem load delivered in grid-connected mode. Third, real-time system information must be available and this requires monitoring and communication infrastructures, such as the GOOSE based system applied in a real industrial project [14]. Lastly, generator protections designed to detect the over/under frequency and voltage conditions are not considered in this paper, i.e. the DG units are assumed to be capable of riding through the abnormal conditions resulting from the fault and the subsequent islanding.

Analytical methods for power system transient assessment are highly complicated, especially for a low-inertia islanded subsystem which is vulnerable to disturbances. Therefore, in this paper, analysis and validations are achieved by repetitive time-domain simulations conducted in PSCAD/EMTDC.

2. System under study

Without considering the energy storage system, at least one conventional synchronous-machine-based DG is essential for an islanded subsystem because it is dispatchable and provides the essential inertia. Consequently, this generator can maintain the stability of the island after losing the main grid. In comparison, an inverter-based DG provides a higher degree of controllability on its output frequency, voltage and power [7], but it is normally intermittent and controlled as a current source.

Fig. 1 shows the layout of an islanding-possible distribution subsystem based on a typical British distribution network consisting of radial feeders [15], the parameters of the system are specified in Appendix A. Formation of the island is initiated by the protective tripping of circuit breaker CB1 (the point of common coupling, PCC), this isolates the subsystem from the upstream fault. The behaviour of automatic reclosers is not considered in this study.

Generation in the subsystem includes a 2 MW diesel-based synchronous DG (DSG) and a 1.5 MVA inverter-based DG (IBG). Subsystem loads consist of static loads and IM loads. A composite 1MVA drive-controlled IM and two composite 1MVA direct-online (DOL) IMs with constant torque and quadratic torque loading respectively are simulated. This paper focuses on load-rich islands, where the island generation capacity is less than the local load demand.

2.1. Diesel-based synchronous DG

The 2 MW DSG was simulated using the standard 5th order synchronous machine model available in the library of PSCAD/EMTDC.

DSG's speed governor and excitation system are also accurately modelled.

A diesel engine drives the synchronous generator and its shaft speed is controlled by a governor, which is represented by a simplified model as shown in Fig. 2. The parameters of the machine and the governor are specified in Appendix A.

In grid-connected mode, the DSG is controlled as a current source (P-Q unit) by leveraging droop control on its governor. When connected to the grid, the DSG is held at a stable frequency and thus its active power output is fixed at the set point. In islanded mode, the DSG is controlled as a voltage source (the V-f unit) and used to maintain the frequency at a fixed level. This requires isochronous control, also known as fixed speed control, i.e. the V-f unit will match its MW power output to the load demand within the island. Proportional (P) and proportional-integral (PI) control are commonly used to realise droop and isochronous control respectively, as seen in Fig. 2.

With respect to the excitation system which grants the voltage regulating ability to the DSG, the AC5A exciter model was adapted from IEEE Std. 421.5-2005 [16]. When operated in grid-connected mode, a fixed amount of reactive power is delivered to ensure the power factor is 0.8. In islanded mode, the DSG's excitation system regulates the subsystem voltage by maintaining the reactive power balanced in the island.

2.2. Inverter-based DG

The primary source of an IBG is normally intermittent renewable energy, such as wind and photovoltaic (PV), which causes unpredictable variations in its MW output. In practice, on-site energy storage, such as flywheels, supercapacitors and batteries, can be installed with this type of DG to eliminate intermittency and ensure constant active power is delivered [17,18]. In this paper, IBG's primary source is assumed to remain unchanged during the islanding switching process, which ensures the IBG can deliver a constant amount of active power to the island through a typical three-leg voltage source inverter.

Vector current control is applied on the inverter to achieve decoupled control of active and reactive power [2,8]. By utilising a synchronous rotating d-q reference frame, the instantaneous active and reactive power can be expressed by a set of two-phase voltages (u_d, u_q) and currents (i_d, i_q). When the d-q frame is aligned to the bus voltage, the power equations can be further reduced to Eq. (1.1) and (1.2).

$$P = u_d i_d + u_q i_q = u_d i_d \tag{1.1}$$

$$Q = u_q i_d - u_d i_q = -u_d i_q \tag{1.2}$$

A double loop control system, as demonstrated in Fig. 3, is used to realise decoupled control [2,8]. The inner current loop generates voltage control signals for pulse-width- modulation (PWM) based on the reference d-q currents (i_{dref} and i_{qref}) obtained from the outer loop. In this paper, the IBG is required to operate as a current source (P-Q unit) in both grid-connected and islanded modes. Therefore, its power outputs must be regulated at the predesigned value and this is achieved in the outer control loop.

2.3. Load model

2.3.1. Static RLC loads

Static loads, including frequency dependency, are modelled using the classical exponential model [19]:

$$P = P_0\left(\frac{V}{V_0}\right)^{n_p}[1 + K_{pf}*(f-f_0)] \tag{2.1}$$

$$Q = Q_0\left(\frac{V}{V_0}\right)^{n_q}[1 + K_{qf}*(f-f_0)] \tag{2.2}$$

where

P_0/Q_0 Rated active/reactive power
V_0/f_0 Rated voltage/frequency
n_p/n_q Voltage index for active/reactive power
K_{pf}/K_{qf} Frequency index for active/reactive power

The static loads used in the following simulations have the aggregate parameter of $n_p = 1$, $n_q = 3$, $K_{pf} = 1$ and $K_{qf} = -1.5$, adapted from [19], and a power factor of 0.9.

2.3.2. Induction Motor (IM) loads

The IM loads consist of a composite 1MVA variable-speed -drive (VSD) interfaced IM and two 1MVA three-phase DOL IMs. Two DOL IMs, adapted from [20], have a constant torque load (a compressor) and a quadratic torque load (a fan) respectively. The VSD IM has a constant torque load. It can operate at various speeds and control the torque and speed in a decoupled manner by using indirect vector control and space-vector PWM technique [21]. All three IMs have a load factor (MW/MVA) of 0.75 and the other parameters are listed in Appendix A.

The IMs are commonly protected against undervoltage conditions by equipping with the motor contactors capable of tripping at around 45–65% of nominal voltage [19,22]. Considering this, the voltage dip up to 50% will be investigated in the following simulations. In addition, the motor stalling protection is also employed to disconnect a motor once its speed reduces to zero.

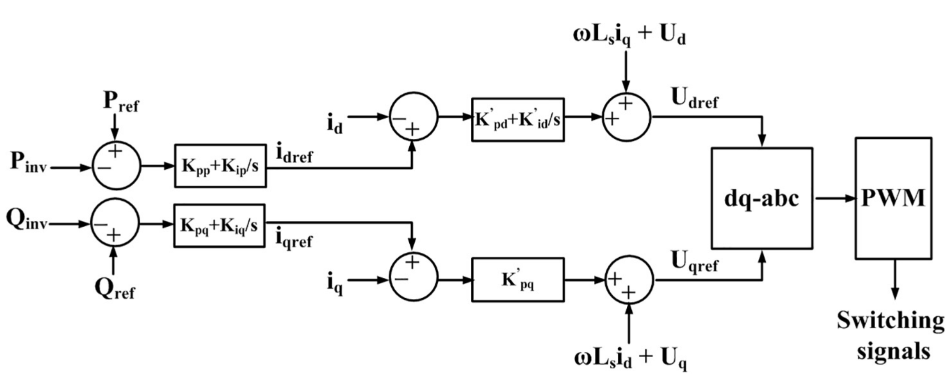

Fig. 3. Double loop control system of IBG (L_S is the filter inductance; U_d/i_d and U_q/i_q are the voltage direct and quadrature components; P_{inv}/Q_{inv} and P_{ref}/Q_{ref} are the real-time and predesigned values of inverter power outputs).

3. Switching control strategy

3.1. DG coordinated control

Base on the ISO-8528-1:2005 standard [23], an AC generator driven by an internal combustion engine normally operates at a load factor of 70% with a power factor of 0.8. Therefore, in grid-connected mode, the DSG is controlled as a P-Q unit to deliver 1.4 MW to the main grid at a power factor of 0.8. This setting gives the DSG a 30% spinning reserve (0.6 MW). The IBG also operates as a P-Q unit and delivers 1.0 MW at a unity power factor in grid-connected mode.

A master/slave scheme was employed to coordinate multiple DGs when operated in islanded mode. Immediately after the islanding switching command, the DSG changes to a V-f unit (master) and regulates the island frequency and voltage. This requires the diesel governor to operate in isochronous mode and the excitation system to be a voltage regulator. In comparison, the IBG continues operating as a P-Q unit (slave) and delivers 1.0 MW to the island. In addition, it is a regular practice for DG inverters to provide reactive power support in an islanded subsystem, which involves changing the power factor within the range of 0.90 lagging to 0.95 leading [24]. Therefore, the IBG is operated at a power factor of 0.90 lagging in islanded mode and injects 0.5MVAr into the island.

3.2. Load shedding algorithm

A low-inertia islanded subsystem is sensitive to power imbalance, and thus fast load shedding is crucial to protect the integrity of the subsystem when the island generation is less than the load. Conventional under frequency load shedding technique is too slow for a low-inertia island, and normally result in overshedding due to its stepwise nature, long processing time and the tripping delay between steps [25]. The use of rate of change of frequency (RoCoF) to estimate the power imbalance is generally considered an effective method, especially in a large-scale power system [26]. But this method usually fails to fully utilise the available spinning reserve, and the estimation is often incorrect especially when the disturbance is severe and transient frequency spikes are experienced [27]. In this paper, the load shedding scheme is designed to quickly shed sufficient load in a single step. The shedding amount is based on the active power flow measured at the PCC immediately before the fault occurs, denoted as P_{PCC}.

P_{PCC} accurately represents the active power deficit in the island, and thus the load shedding decision is quickly made after the disturbance, to achieve minimum processing time. The other reason of using P_{PCC} is to facilitate the application of distributed control. Compared to centralised load shedding schemes in [26,27], distributed schemes can effectively reduce the communication delay by getting rid of the remote control centre, which enhances system reliability and decision-making efficiency [28,29]. This scheme relies on the intelligent electronic device (IED) installed at the PCC as the master unit to collect the real time system data from the other slave IEDs locating at the generator and the load sites. Once the islanding occurs, the master IED can quickly determine the loads that need to be shed, based on P_{PCC} and the latest system data, as updated immediately before the disturbance. Afterwards, control commands will be allocated to the corresponding slave IEDs to implement load shedding.

The actual load shedding amount (P_{LS}) is depicted as:

$$P_{LS}\ (\mathrm{MW}) \geqslant P_{PCC} - Spinning\ Reserve - \Delta Loss \tag{3}$$

$\Delta Loss$ is the loss deviation before and after islanding. In the simulated island, the system loss is deliberately controlled to zero, i.e. $\Delta Loss$ is zero. While $\Delta Loss$ can also be neglected in practice, because it is usually small and impossible to be measured in real time. Neglecting $\Delta Loss$ results in over-shedding which is beneficial because it not only enhances the transient stability due to larger generation reserve [8] but also provides a safety margin when the subsystem operates in islanded mode.

Spinning reserve is the spare active power available at the dispatchable generation in the island. This data is continuously measured and transmitted to the decision-making IED (located at the PCC). Therefore, it is visible, along with the P_{PCC}, when the load shedding amount is calculated. *Spinning reserve* in this paper is equal to the spare MW capacity of the DSG, i.e. 30% of its capacity = 0.6 MW.

The other important aspect of a load shedding scheme is the load priority. To determine a proper priority, the transient behaviour of different types of load should be analysed and this will be demonstrated in the next section.

4. Transient analysis

The islanded subsystem is assumed to be load-rich, and the scenarios with 80/60/40% of DG penetration level are next examined. DG penetration represents the proportion of the dispatchable island generation (3MW) to the total subsystem on-grid load. For these scenarios, the switching control is executed 300 ms after the formation of the island. This control delay is used to demonstrate the islanding detection time, the algorithm processing time and the communication delay.

4.1. DG penetration = 80% (on-grid load = 3.75 MW)

An island is formed at $t = 3.0$ s following a 10% voltage dip event resulting from a single-phase fault at $t = 2.5$ s. This is translated to a fault clearance time (FCT) of 500 ms which is the typical value used in a 11 kV distribution network [30].

After the execution of the switching control, a successful islanding switching is achieved, as presented in Fig. 4. In this scenario, all IM loads are continuously powered while a portion of the static loads is shed to maintain the load-generation balance. The P_{PCC} measurement at $t = 2.49$ s is 1.35 MW, and the load shedding amount, calculated from (3), is 0.75 MW.

Fig. 4 shows the system voltage rapidly drops at $t = 2.5$ s due to the fault but starts recovering after the execution of the switching control at $t = 3.3$ s. During the fault period, the system frequency remains stable since the main grid is still connected and strong enough to handle the system load decreasing caused by the voltage dip. However, once the subsystem is isolated from the main grid, the system frequency keeps declining due to the active power deficit until the implementation of the load shedding.

The transient responses of different types of DG units are illustrated in Fig. 4(c). Before islanding, the DSG is a P-Q unit delivering fixed 1.4 MW power at a power factor of 0.8, but it is switched to the V-f unit in islanded mode to regulate the system frequency and voltage. The IBG maintains a fixed 1 MW power output in both modes and it is able to rapidly restore the stability after the disturbances. As seen in Fig. 4(e) and (f), the powers of DOL IMs (compressor and fan motors) are roughly voltage dependent, similar to the static loads, and their speeds follow the system frequency. In comparison, the VSD IM consumes effectively constant power and maintains constant speed regardless of the system frequency.

When experiencing a severe voltage dip, DOL IMs, especially the compressor motor which has small inertia (H = 0.2 s) and constant torque loading, are likely to lose stability and stall, unless the FCT is very short [8,13]. The stalled IM will draw a large amount of power from the system [22], and thus seriously threatens the island stability.

Fig. 5 shows the case where a 50% voltage dip is caused by a phase-phase fault and the motor undervoltage protection is not triggered. As observed in Fig. 5(d), if the FCT remains at 500 ms, the compressor motor keeps decelerating following the severe voltage dip and fails to

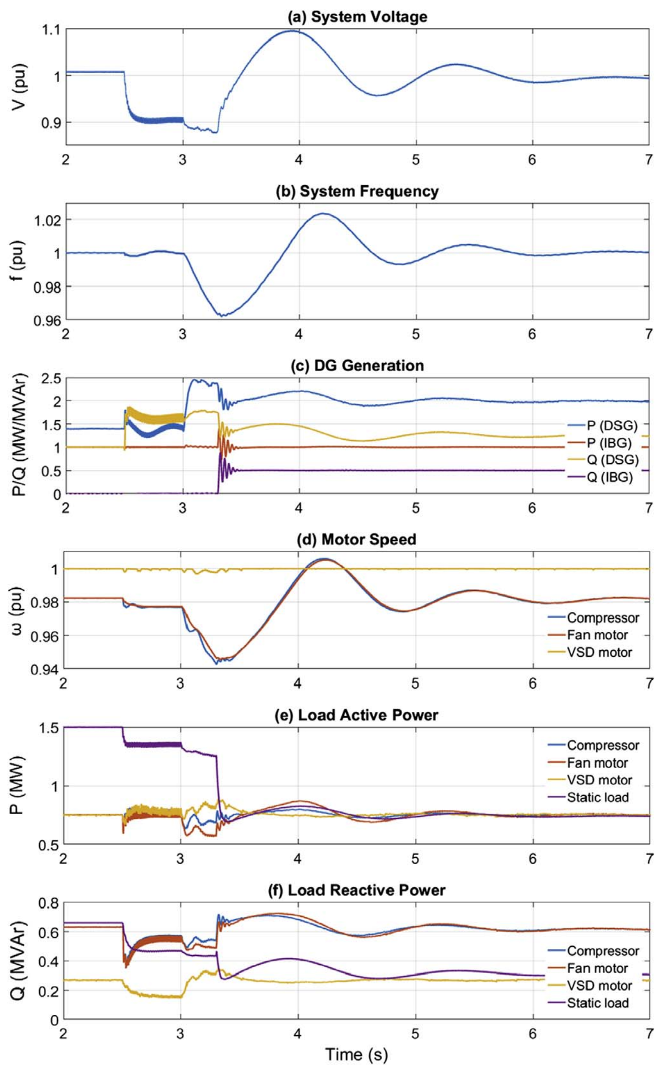

Fig. 4. Switching transients of scenario_1 (single-phase fault).

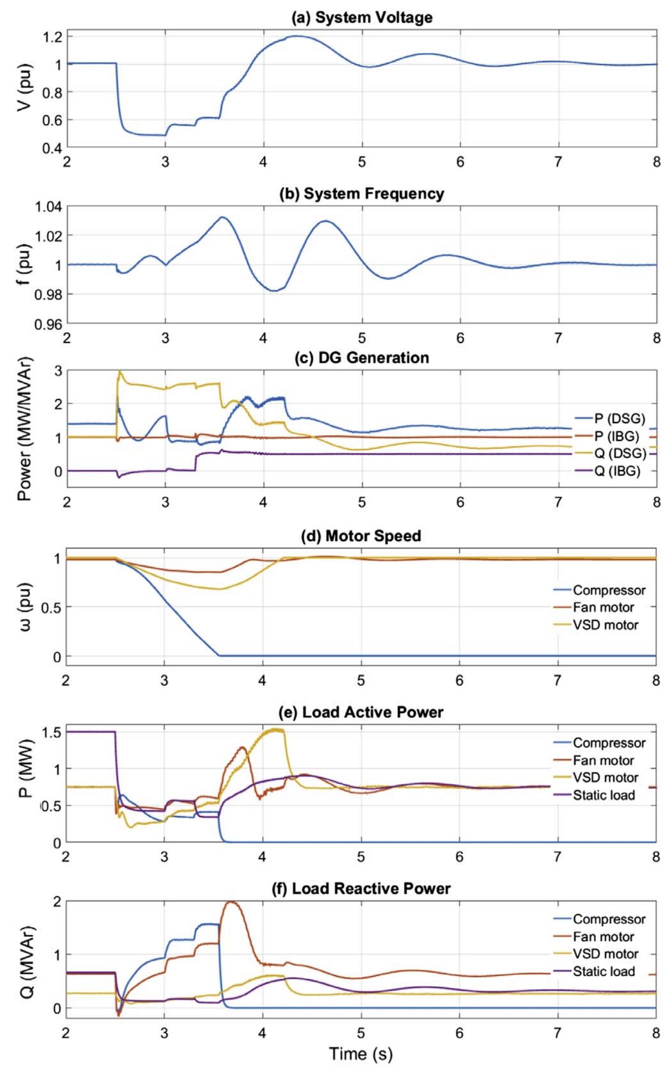

Fig. 5. Switching transients of scenario_1 (phase-phase fault).

reaccelerate even after the voltage is restored, i.e. it stalls. Finally it is tripped by the IM stalling protection at $t = 3.5$ s. If the compressor motor must stay powered, the FCT must be further reduced to 190 ms to prevent motor stalling.

A stalled motor consumes significant MVAr, and this may prevent the voltage recovery considering the limited MVAr capacity of an island. The motor acceleration also demands extra MVAr, and thus the recovery of the other IMs can only happen after the disconnection of the compressor motor. It is also noticed that a motor consumes extra MW at the end of its acceleration in consistent with the speed-torque characteristic. Therefore, keeping the IM loads connected in the island degrades the switching transients and might even lead to an unsuccessful switching if the stalled motor is not tripped.

The frequency rise is also observed after islanding despite the island is designed as load-rich. This is because the low voltage massively reduces the total load MW, as seen in Fig. 5(e), and results in a generation-rich condition.

Assuming the motor's undervoltage protection is disabled or it fails to operate on a severe voltage dip, the system transients following a three-phase fault is demonstrated in Fig. 6. As observed in the figure, an 80% voltage dip is induced by the fault which massively decreases the island load MW and creates a large generation surplus during the fault period. This voltage dip also rapidly slows down the IMs and causes the compressor motor stalling.

After islanding, because the stalled compressor motor is quickly tripped at $t = 3.1$ s, the system recovers and eventually stabilises. Under such a fault condition, the FCT must be very short if the compressor motor stays connected. Table 1 lists the maximum FCT required for the compressor motor to survive the fault and following islanding period.

As seen in the table, the FCT required for the successful islanding switching is very short, particularly when a severe voltage dip event is experienced. Because it is impractical to adopt such a short FCT on an 11 kV distribution network, the load shedding priority needs to be re-evaluated according to the load stability issues discovered in the above simulations.

(1) *Static Load:* In consistent with (2.1), the MW consumption of a static load is majorly voltage dependent. This dependency benefits the system recovering process.
(2) *DOL IM Load:* The voltage dip causes the flux of the DOL IM to rapidly drift down, which reduces the developed torque and consequently decreases the motor speed and the consumed power [12]. Once the fault is cleared and the system voltage restores, the unstalled IMs slowly recover to the nominal operation. During the

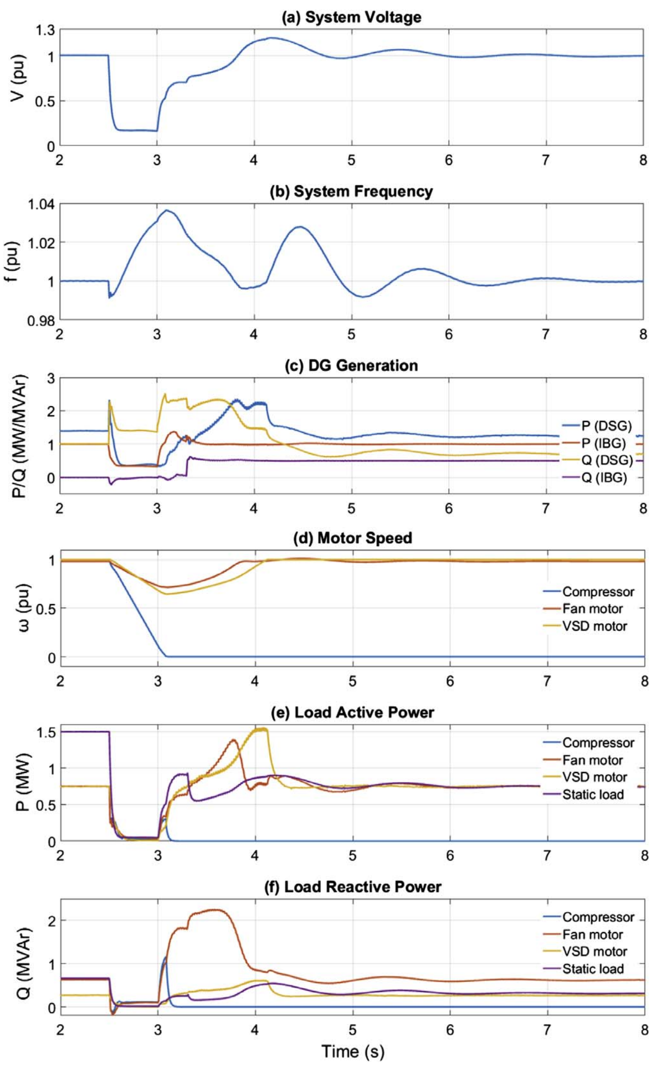

Fig. 6. Switching transients of scenario_1 (three-phase fault).

Table 1
Maximum FCT required for successful islanding switching.

Voltage dip (%)	Maximum FCT (ms)
39	500
50	190
60	120
70	70
80	40

recovery, IMs absorb significant power to reaccelerate the rotor, as shown in Figs. 4–6. The severer the voltage dips, the more the motor speed declines which then requires a longer time to reaccelerate. In Figs. 5 and 6, when a prolonged and deep voltage dip is experienced, the DOL compressor motor keeps losing speed and cannot accelerate even on the restoration of the supply voltage, i.e. the motor stalls. The stalled motor is harmful to the island stability and must be disconnected rapidly. Therefore, if the stalling protection is slow or fails to operate, the stalled motor must be shed by the load shedding scheme.

(3) *VSD-Interfaced IM Load:* The application of a VSD decouples the motor speed with the grid frequency. Because of this, the transient stability of VSD IMs is much stronger than the DOL IMs. Figs. 5 and 6 show, with the same constant torque loading, the VSD IM survives the severe faults while the DOL IM loses stability and stalls. The power and speed of a VSD IM can be maintained stable during both the fault and the islanding switching periods. A VSD also raises the power factor of the motor current and leads a VSD IM to demand mainly MW power when it accelerates.

Base on the discussions above, IM loads are less preferable to stay connected during the islanding switching since they consume significant power to reaccelerate which may degrade the system transients. Typically for a severe fault event, DOL IMs with constant torque loading must be shed to prevent motor stalling, but this may not be necessary if rapid fault clearance is achievable. Consequently, the load shedding priority, in terms of the load transient performance, can be designed as “DOL IM (constant torque loading) > DOL IM (quadratic/linear torque loading) > VSD IM > Static load”.

4.2. DG penetration = 60% (on-grid load = 5.0 MW)

Based on the designed load shedding priority, in this subsection, the DOL compressor motor is shed in the double- or three-phase fault cases. While in the single-phase fault case, the compressor stays connected during the switching process to study the worst case scenario. Simulation results are illustrated in Figs. 7 and 8 respectively with a 500 ms FCT. The P_{PCC} measurement at $t = 2.49$ s is 2.6 MW, and the load shedding amount, calculated from (3), is 2.0 MW.

Fig. 7 depicts a smooth islanding switching following a single-phase fault. But compared to the scenario_1 with a higher DG penetration, as shown in Fig. 2, the frequency and voltage transients are degraded in this scenario. The IMs also slow down more severely and consume more power during reacceleration. This is because a higher power deficit is seen in the island before the implementation of the load shedding.

For the phase-phase fault case as illustrated in Fig. 8, unlike the maximum 190 ms FCT required when the compressor motor keeps connected in the island, a significantly slower FCT, such as 500 ms, can be adopted when this motor is shed. Therefore, applying this shedding priority is necessary. The frequency deviation in Fig. 8 is considerably smaller than that in Fig. 7. This is because the reduction of the load MW, due to the severe voltage dip, prevents the fast frequency decline. As seen in Fig. 8(e), after the load shedding, the remaining IMs reaccelerate and consume extra amount of MW, which decreases the system frequency. Once the IM acceleration is finished at $t = 4$ s, the MW consumption of IMs immediately drops and this creates an instant generation surplus resulting in a noticeable frequency overshoot.

4.3. DG penetration = 40% (on-grid load = 7.5 MW)

The P_{PCC} measurement at $t = 2.49$ s is 5.1 MW, and the total load shedding amount, calculated from (3), is 4.5 MW. When the designed load shedding scheme is applied, the transient voltage and frequency responses are shown in Fig. 9, along with these results obtained from aforementioned scenarios. This comparison demonstrates the impact of the DG penetration level on the islanding switching transients.

The result indicates that the proposed control strategy is effective in ensuring successful islanding switching with the DG penetration level varying from 40% to 80%. It also validates that the typical FCT of 500 ms is appropriate for these cases. Fig. 9(a) and (b) show that the transient response during a single-phase fault initiated islanding is significantly affected by the DG penetration level. This is because a higher DG penetration implies a smaller MW deficit in the island which mitigates the frequency decline during $t = 3$–3.3 s. The frequency rising

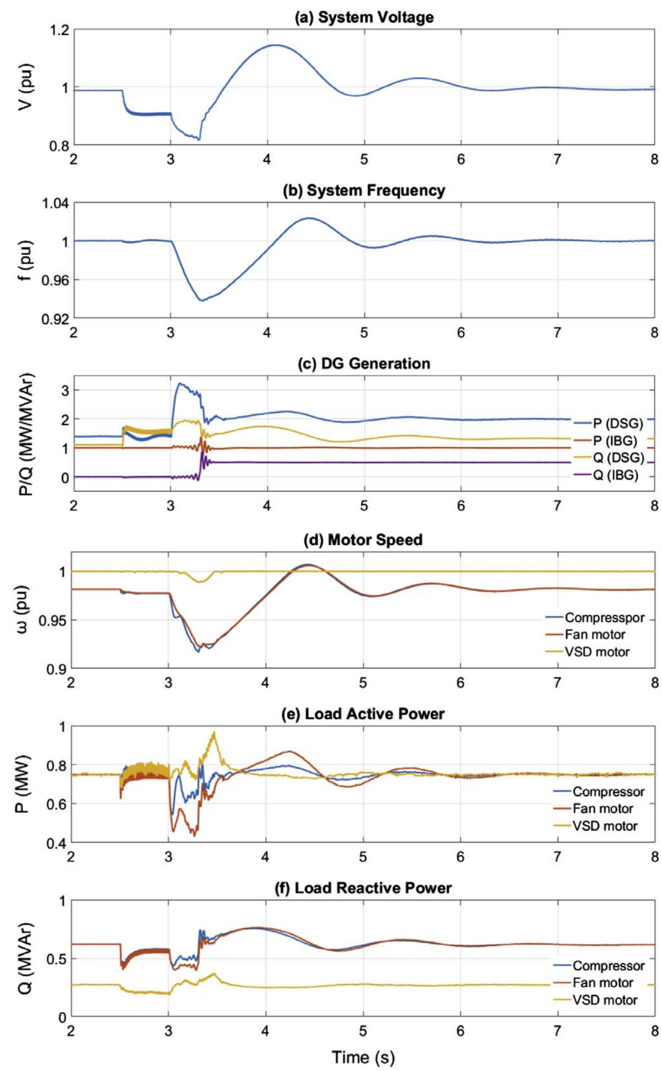

Fig. 7. Switching transients of scenario_2 (single-phase fault).

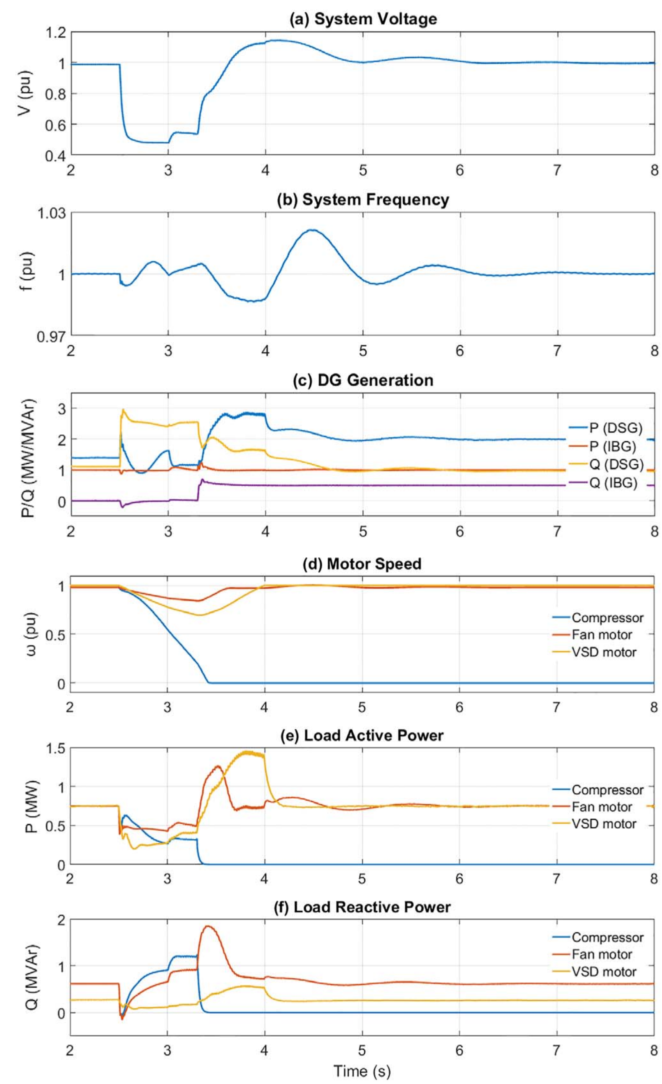

Fig. 8. Switching transients of scenario_2 (phase-phase fault).

speed is the same in all cases since the maximum mechanical torque available at the synchronous generator to accelerate its rotor is fixed. A smaller voltage dip and less overshoot are also experienced in the high DG penetration case because the excitation system has a lower MVAr deficit to balance.

When the islanding is initiated by a phase-phase fault, the island load MW demand is significantly lowered by the severe voltage dip. This results in a frequency increase during t = 3–3.3 s in the cases with high DG penetration levels, as seen in Fig. 9(d). After the load shedding execution, the system voltage sharply rises and this increases the load MW at the same time. Consequently, a quick frequency decline is observed considering the synchronous generator takes time to ramp up its mechanical MW output to match the increasing load MW demand. The other frequency rise during t = 4–4.5 s is because the MW demand from IM loads suddenly drops at the end of their acceleration process.

According to the existing power quality requirements, the operating frequency of an islanded subsystem, with no synchronous interconnection, is 50 Hz ± 2% [31], and the voltage deviation range in European industries is −15%/+10% [32]. Therefore, the system settling time can be defined as the time when the subsystem recovers within these ranges. As seen in Fig. 9(a) and (b), a higher DG penetration can effectively decrease the settling time. However, for phase-phase fault cases, the frequency deviations are similar, and they are kept within the acceptable range during the entire process.

5. Impact of switching control delay

In aforementioned case studies, the time delay required to execute the switching control is 300 ms after the formation of the island, which is proved to be appropriate in all scenarios. This control delay is used to demonstrate the presence of the islanding detection time, the decision making time, the communication delay and the circuit breaker opening time. In this section, the impact of switching control delay on the system transient performance is examined. The scenario with 60% DG penetration level is taken as the example.

5.1. Single-phase fault case

As observed in Fig. 10, the islanded system successfully recovers and the recovery responses are identical in all cases. A faster control execution can promise a better power quality by effectively reducing the frequency and voltage deviation. However, if the control execution is

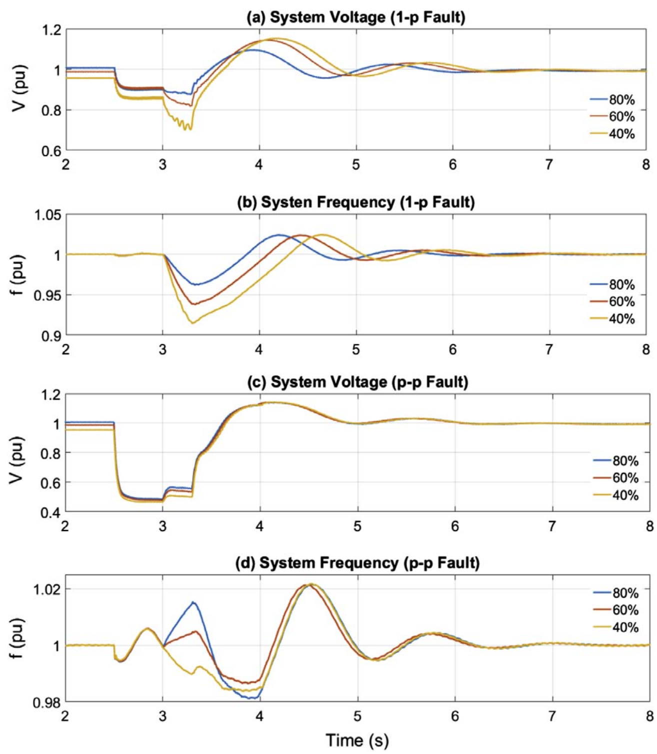

Fig. 9. Impact of DG penetration level.

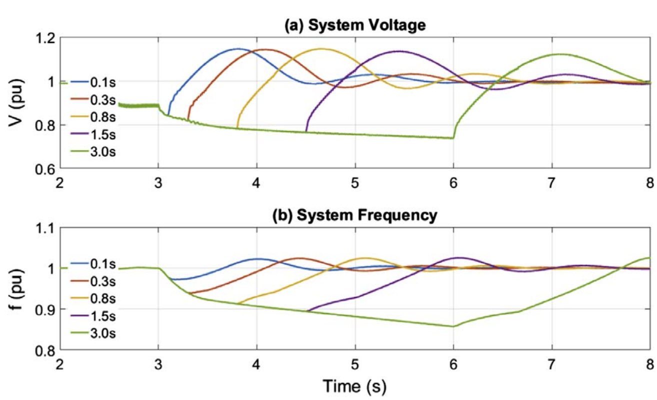

Fig. 10. Impact of switching control delay (single-phase fault).

further delayed, as seen in Fig. 11, the system becomes unstable at $t = 9.2$ s and fails to recover even after the control execution at $t = 10.0$ s. This is because the IM parameters become unstable with large oscillations once the motor speed declines too low, and consequently the system frequency and voltage becomes oscillating. Therefore, the switching control must be executed fast enough to restore the motor speed to an acceptable value. In addition, since the operation in low frequency and low voltage may damage the electric devices, such as motors, power electronics and generators. The switching control needs to be executed as rapidly as possible.

5.2. Phase-phase fault case

Figs. 12 and 13 indicate the system can survive the fault and the subsequent islanding even though the switching control is executed slowly. Before the control execution, the island stabilises at an unacceptable condition with a low voltage and a low frequency. Due to the increased MVAr consumed by the IMs when operating at low speeds, the DGs have insufficient MVAr capacity to restore the voltage. Consequently, this low voltage results in a decrease in the total island load MW demand, and the island load-generation can be balanced at a low level. During this period, instead of keeping losing speed as seen in

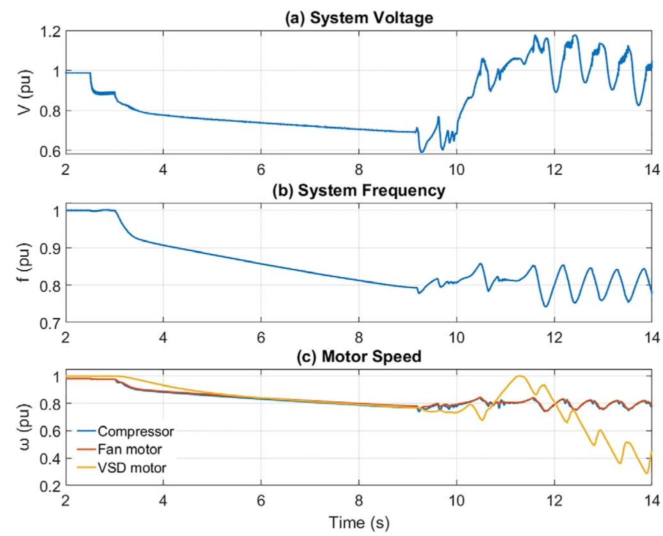

Fig. 11. System transients with a long control delay (single-phase fault).

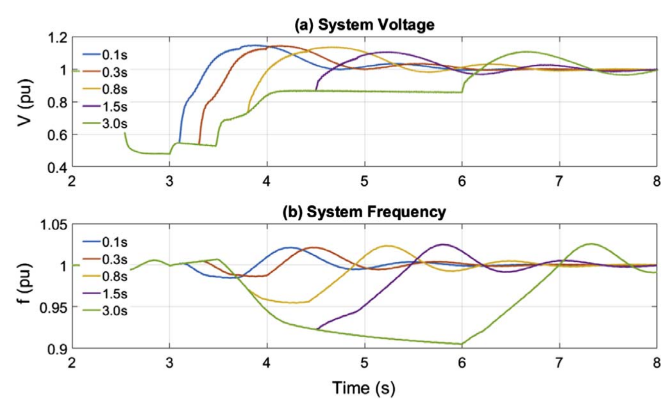

Fig. 12. Impact of switching control delay (phase-phase fault).

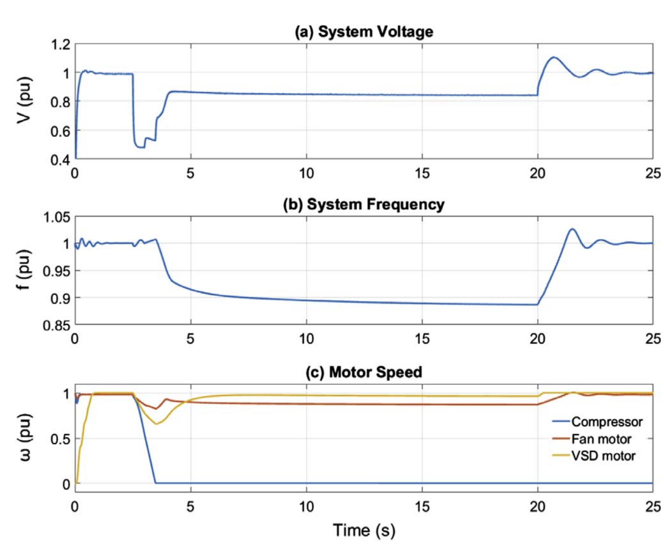

Fig. 13. System transients with a long control delay (phase-phase fault).

the single-phase fault case, the remaining IM loads are able to operate at low speeds.

Once the switching control is executed, the frequency and voltage immediately start recovering and the recovery transients are almost identical in all cases. Therefore, the appropriate control speed should also consider the system protection settings. The maximum time delay before the protection operates to trip system components, such as generator or load tripping due to the undervoltage protection, determines the slowest speed allowed for the switching control execution.

6. Conclusion

The transient stability of a distribution subsystem during the fault-forced switching to islanded operation was studied in this paper. A load-rich subsystem that consists of multiple DGs and various types of load was investigated. To ensure a successful islanding switching with acceptable frequency and voltage transients, a control strategy including a DG control coordination method and a single-step load shedding scheme was designed.

When the subsystem operates in islanded mode, the diesel-based synchronous DG was the master unit regulating the system at a frequency of 50 Hz and at an appropriate voltage, while the inverter-based DG was controlled as the slave to deliver constant power. In addition, a load shedding scheme was presented to maintain the load-generation balance in the island. The load shedding amount was calculated based on the real time P_{PCC} measurement and the *spinning reserve* available at the dispatchable DGs which together can effectively describe the power deficit in the island.

The load shedding priority was the other critical part of a load shedding scheme. In this paper, this priority was determined in terms of the load transient stability. According to the simulation results, the static load and the VSD-interfaced IM load can withstand severe fault conditions using the typical 500 ms FCT, while the DOL IM load might lose stability and stall unless an extremely short FCT is available. Therefore, the DOL IM loads, especially those with small inertia and constant torque loading, must be shed if a severe voltage dip is experienced. Therefore, the load shedding priority is finally designed as "DOL IM (constant torque loading) > DOL IM (quadratic/linear torque loading) > VSD-interfaced IM > Static load".

The impacts of the DG penetration level and the switching control delay were also examined. The result shows both factors significantly affect the system transient performance during the islanding switching process. Generally speaking, a higher DG penetration can improve the transient performance by decreasing the frequency/voltage deviations and the system settling time. The switching control must be executed fast enough to prevent the system collapsing, but a proper control speed should also consider the power quality requirements and the system protection settings. The control must be executed before the unqualified frequency or voltage damages the system components.

Appendix A

Utility network represented by Thevenin equivalent model:

33 kV, 1000 MVA and source impedance = 1.089 Ω; Grounding resistor = 6 Ω (ground fault current limiter).

Transformer parameters:

Voltage ratio (kV)	Base (MVA)	R (pu)	X (pu)	Windings
33/11	10	0.005	0.06	Yyn
11/0.4	5	0.01	0.05	Dyn11

Diesel governor:

Proportional gain (droop mode): 20;
Proportional gain (isochronous mode): 40;
Integral time constant (isochronous mode): 0.015;
Fuelling actuator time constant: 0.2 s;
Engine dead time: 0.024 s;
Fuelling factor (K_F): 1.

Synchronous generator:

Rated capacity: 2.5 MVA;
Base angular frequency: 50 Hz;
Inertia constant: 1.48 s;
Armature resistance (R_a): 0.01 pu;
Leakage resistance (R_L): 0.135 pu;
Direct axis reactance (X_d): 2.65 pu;
Transient direct axis reactance (X_d'): 0.22 pu;
Sub-transient direct axis reactance (X_d''): 0.15 pu;
Quadrature axis reactance (X_q): 2 pu;
Sub-transient quadrature axis reactance (X_q''): 0.25 pu.

Induction motor:

4-pole squirrel cage induction machine;
Load Factor (MW/MVA): 0.75;

Stator resistance: 0.009 pu;
First cage resistant: 0.139 pu;
Second cage resistant: 0.026 pu;
Stator unsaturated leakage reactance: 0.052 pu;
Unsaturated magnetizing reactance: 1.993 pu;
Second cage unsaturated reactance: 0.113 pu;
Inertia constant: 0.2 s (Compressor), 0.5 s (Fan).

Reference

[1] Jayaweera D, Galloway S, Burt G, McDonald JR. A sampling approach for intentional islanding of distributed generation. IEEE Trans Power Syst 2007;22:514–21.
[2] Balaguer IJ, Lei Q, Yang S, Supatti U, Peng FZ. Control for grid-connected and intentional islanding operations of distributed power generation. IEEE Trans Ind Electron 2011;58:147–57.
[3] IEEE standard for interconnecting distributed resources with electric power systems. IEEE Std 1547–2003; 2003. p. 1–28.
[4] Meliopoulos APS. Challenges in simulation and design of micrograds. IEEE power engineering society winter meeting conference proceedings, vol. 1. 2002. p. 309–14.
[5] IEEE guide for design, operation, and integration of distributed resource island systems with electric power systems. IEEE Std 15474-2011; 2011. p. 1–54.
[6] Shahabi M, Haghifam MR, Mohamadian M, Nabavi-Niaki SA. Microgrid dynamic performance improvement using a doubly fed induction wind generator. IEEE Trans Energy Convers 2009;24:137–45.
[7] Katiraei F, Iravani MR, Lehn PW. Micro-grid autonomous operation during and subsequent to islanding process. IEEE Trans Power Deliv 2005;20:248–57.
[8] Alaboudy AHK, Zeineldin HH, Kirtley J. Microgrid stability characterization subsequent to fault-triggered islanding incidents. IEEE Trans Power Deliv 2012;27:658–69.
[9] Raj PA, Sudhakaran M. Optimum load shedding in power system strategies with voltage stability indicators. Sci Res Eng J 2010;2.
[10] Mahat P, Chen Z, Bak-Jensen B. Underfrequency load shedding for an islanded distribution system with distributed generators. IEEE Trans Power Deliv 2010;25:911–8.
[11] Ding Z, Cartes DA, Srivastava S. New load shedding scheme for islanded power systems. IEEE/SMC international conference on system of systems engineering. 2006. p. 6.
[12] Milanovic JV, Aung MT, Vegunta SC. The influence of induction motors on voltage sag propagation – Part I: Accounting for the change in sag characteristics. IEEE Trans Power Deliv 2008;23:1063–71.
[13] Liu Y, Vittal V, Undrill J, Eto JH. Transient model of air-conditioner compressor single phase induction motor. IEEE Trans Power Syst 2013;28:4528–36.
[14] Adamiak M, Schiefen MJ, Schauerman G, Cable B. Design of a priority-based load shed scheme and operation tests. IEEE Trans Ind Appl 2014;50:182–7.
[15] Ingram S, Probert S, Jackson K. The impact of small scale embedded generation on the operating parameters of distribution networks. UK: Department of Trade and Industry; 2003.
[16] IEEE recommended practice for excitation system models for power system stability studies. IEEE Std 4215-2005; 2005.
[17] Cardenas R, Pena R, Asher G, Clare J. Power smoothing in wind generation systems using a sensorless vector controlled induction machine driving a flywheel. IEEE Trans Energy Convers 2004;19:206–16.
[18] Abbey C, Joos G. Short-term energy storage for wind energy applications. Fourtieth IAS annual meeting conference record of the 2005 industry applications conference. 2005. p. 2035–42.
[19] IEEE Task Force on Load Representation for Dynamic Performance. Load representation for dynamic performance analysis. IEEE Trans Power Syst 1993;8:472–82.
[20] Pedra J, Sainz L. Parameter estimation of squirrel-cage induction motors without torque measurements. IEE Proc – Electr Power Appl 2006;153:263–70.
[21] Vas P. Vector control of AC machines. New York: Clarendon Press; 1990.
[22] North American Electric Reliability Corporation. Dynamic load modeling technical reference document; 2016. Available: < http://www.nerc.com/comm/PC/LoadModelingTaskForceDL/Dynamic%20Load%20Modeling%20Tech%20Ref%202016-11-14%20-%20FINAL.PDF > .
[23] Reciprocating internal combustion engine driven alternating current generating sets – Part 1: Application, ratings and performance; 2005.
[24] Ellis A, Nelson R, Engeln EV, Walling R, MacDowell J, Casey L, et al. Reactive power performance requirements for wind and solar plants. 2012 IEEE power and energy society general meeting. 2012. p. 1–8.
[25] Tofis Y, Timotheou S, Kyriakides E. Minimal load shedding using the swing equation. IEEE Trans Power Syst 2017;32:2466–7.
[26] Terzija VV. Adaptive underfrequency load shedding based on the magnitude of the disturbance estimation. IEEE Trans Power Syst 2006;21:1260–6.
[27] Seyedi H, Sanaye-Pasand M. New centralised adaptive load-shedding algorithms to mitigate power system blackouts. IET Gener Transm Distrib 2009;3:99–114.
[28] Zhang Z, Chow MY. Convergence analysis of the incremental cost consensus algorithm under different communication network topologies in a smart grid. IEEE Trans Power Syst 2012;27:1761–8.
[29] Xu Y, Liu W, Gong J. Stable multi-agent-based load shedding algorithm for power systems. IEEE Trans Power Syst 2011;26:2006–14.
[30] Electricity North West UK. System earthing and fault levels. Available: < http://www.enwl.co.uk/about-us/long-term-development-statement/policies-and-technical-references/system-earthing-and-fault-levels > .
[31] Baggini A. Handbook of power quality. West Sussex, England: John Wiley & Sons Ltd.; 2008.
[32] The European Regulators Group for Electricity and Gas (ERGEG). Towards voltage quality regulation in Europe. Bruxelles; 2007.